CO_2 Glaciers on the South Polar Layered Deposits of Mars. I. B. Smith[1,2]; E. Larour[3]; N. E. Putzig[2]; R. Greve[4]; N. Schlegel[3], Ignacio Isola[1]. [1]York University, Toronto, Ontario, [2]Planetary Science Institute, Denver, Co; [3]Jet Propulsion Laboratory, Pasadena, Ca; [4]Hokkaido University, Sapporo, Japan Contact: ibsmith@yorku.ca.

Introduction: A thin unit of CO_2 ice, called the south polar residual cap (SPRC), overlies the south polar layered deposits (SPLD) of Mars. This unit, capping a domed-shaped ice deposit, has inspired several studies concerning the glacial-like flow of CO_2 ice under martian conditions [1-3]. Furthermore, evidence of moraines at the north pole have led to interpretations that CO_2 ice was once prevalent there and that it flowed [4]. However, prior to 2011, no known and present day deposits were thick enough to flow.

After 2011 data from the Shallow Radar (SHARAD) instrument on Mars Reconnaissance Orbiter were used to determine that massive CO_2 deposits are buried beneath the surface of the SPRC [5]. Using geophysical arguments and layer geometry, [5] and then [6 and 7] determined that CO_2 ice up to 1000 m thick had been deposited in the spiral depressions of the SPLD before being buried. A total of 16,500 km^3 is likely stored there, having been deposited in three distinct periods. This interpretation re-opened the door for the massive CO_2 deposits to undergo viscous flow.

Laboratory experiments have determined that CO_2 ice is much less viscous than water ice at similar temperatures (150-170 K), by up to two orders of magnitude [1,2], and therefore it must flow much more readily. More recent experiments have been conducted over a wider range of temperatures and grain sizes, and while the stiffness of CO_2 has been refined upward (making it more viscous), there is still a large difference between that value and the value for H_2O [8]. Thus, the thick CO_2 ice deposits are likely to flow.

Observations: Using Mars Orbiter Laser Altimeter topography (MOLA) [9], we identify three distinct gross morphologies that support the flowing ice hypothesis (Fig 1). A thin dome of CO_2 ice resides near the highest point on the SPLD. At the lowest elevations, the CO_2 deposits have surfaces that are nearly perfectly flat, and at intermediate elevations, where the ice fills spiral depressions [7], topographic profiles and contours resemble those of alpine glaciers on Earth. Additionally, there are numerous secondary features, such as compression ridges and crevasses, that indicate flow informed the present state of the glaciers. These will be presented at LPSC 2020.

Table 1: Model Inputs.

Heat Capacity CO_2	700 J/K
Thermal Conductivity	0.4 W/m/K
Geothermal Flux	0.020 W/m^2
Current Surface Temp	150 K
Higher Surface Temperature	170 K

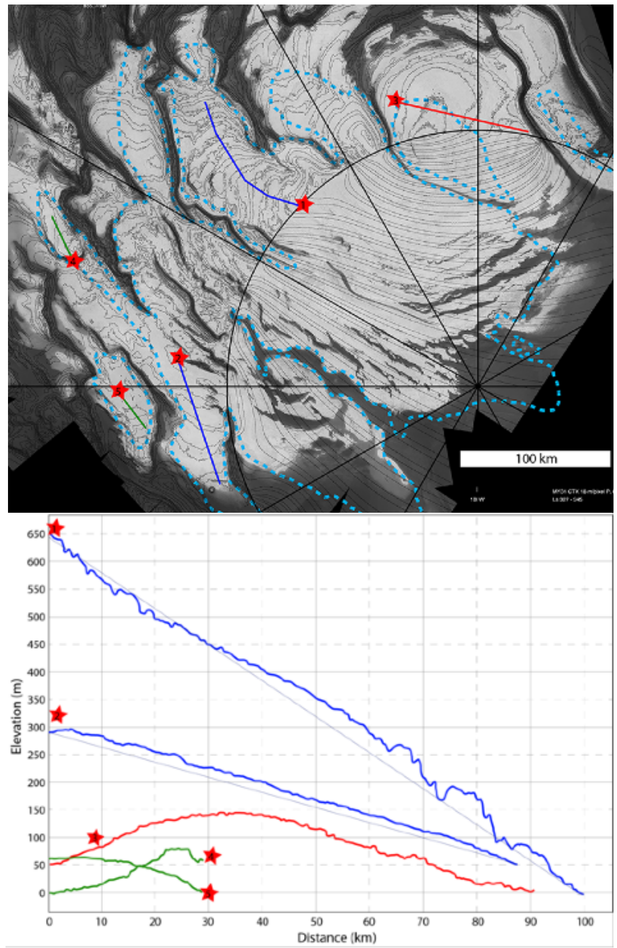

Figure 1: *Relative topography and contours of SPLD CO_2 deposits: above) 40 m contour lines [from 9] over a south polar summer mosaic* [10]. *Topographic profiles in lower panel correspond to colored lines; below) topographic profiles corresponding to colored lines above. Observations can be categorized by three groups: dome shaped topography (red), convex up 'alpine style' glaciers (blue), and nearly flat topography (green). Straight lines show slope context.*

Modeling: To assess the current flow and the circumstances that caused the ice deposits to reach their present state, we employ the Ice Sheet System Model (ISSM) [11]. ISSM successfully simulates glaciers and ice sheets on Earth and can be adapted to Mars by changing parameters for the planet (e.g. geothermal flux, gravity) and for the type of ice (eg. rheological parameters, thermal conductivity) (Table 1). A very high friction coefficient was chosen to prevent basal sliding because CO_2 glaciers are dry based. Full thermal conduction and advection is included with the model.

Following [3], we choose a Glen's law behavior using this equation and inputs from [8]:

$$\dot{\varepsilon} = A\sigma^n e^{(-Q/RT)}$$

Where $\dot{\varepsilon}$ is strain rate, A is a material constant (A= $10^{13.4}$ MPa^{-n}/s), Q is the activation energy (Q = 68.2 kJ/mol), R is the gas constant ($R_{(gas)}$ = 8.3144598 J/K/mol), and n is the stress exponent (n=8).

To assess the current state, we input the surface topography [9], deposit thickness and basal topography [7], and surface temperature (locked at ~150 K, the sublimation temperature of CO_2 in Mars conditions) and run a steady state simulation that calculates the vertical temperature profile of the deposits and then all of the stresses and strains of the present-day features. These simulations can be run in minutes.

To determine the duration of time required to reach the present state, we begin with the basal topography [7] and run forward simulations that begin with no CO_2 ice but have a positive surface mass balance (SMB) of 0.01 m per year for a total of 200 kyr over a small region. We allow the deposits to relax over an additional 300 kyr. For these long duration simulations, we cropped the domain to reduce running time. In the smaller domain, each 100 kyr takes about 24 hours of clock time. The SMB was confined to a small location near the highest elevation of the domain.

Results: Here, we present only the forward model "transient" simulations. The velocity of the ice deposits are most strongly affected by surface slope, and in our model this is driven by the distribution of SMB and the slope over which the ice flows. Over the course of 200 kyr of accumulation and 300 kyr with 0 SMB, the velocity changes by a factor of ~2.5.

During accumulation, the maximum velocity exceeds 0.4 m/year. After accumulation, the velocity decreases secularly to ~0.2 m/year until the ice flows beyond the confines of a spiral depression, spilling over into another trough, when the velocity increases rapidly. The final state (Fig 2) resembles the current topography qualitatively, even given the unrealistic SMB distribution.

Discussion: After 500 kyr, our forward, transient simulations result in surface topography and glacier thickness similar to that observed with radar, supporting the hypothesis that the CO_2 deposits are flowing today at a velocity <20 cm/year. The ice will flow greatest during periods of accumulation and then settle to lower speeds once accumulation ceases. Flow durations > 500 kyr may be unlikely because the ice would have flowed farther than the current distribution would allow (over the edge of the SPLD), possibly providing a constraint on how long the ice has been present.

Because the SMB distribution was unrealistic, and because the final result was so similar to actual Mars, we argue that the SMB distribution is not the most important factor in how the glaciers evolve to their present state. Thus, the bed topography and the slopes between troughs drive ice flow into the current form. The reduced importance of SMB distribution may make ascertaining the depositional history difficult.

Because surface mass balance (rate, not necessarily distribution) is one of the two greatest factors that influence flow velocity, we interpret these results to mean that while the CO_2 deposits are likely flowing now, the rate is slower by at least a factor of two from previous epochs, when accumulation took place.

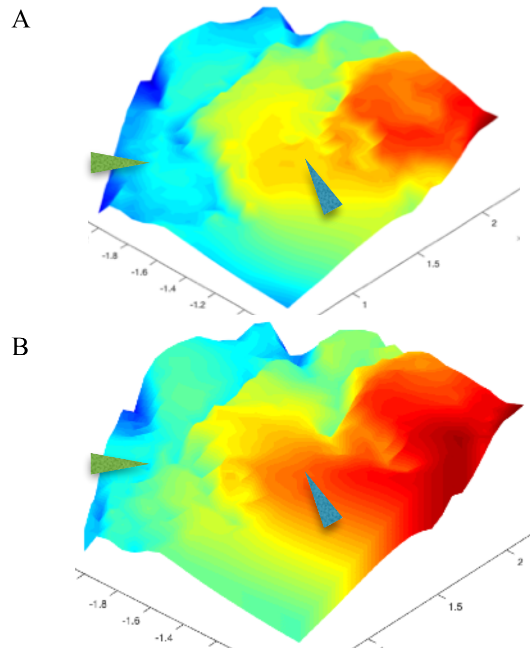

Figure 2: *Perspective views of topography. A) Simulation after 500 kyr of flow (200 kyr of accumulation (near blue arrow tip) followed by 300 kyr of flow without accumulation. Notice that the lower trough (green arrow) fills in after the ice spills over from the upper trough (blue arrow). B) Current Mars topography. Blue arrows indicate flow direction. Qualitatively, these are very similar, and the location of accumulation has little effect on the final result.*

Future work: The CO_2 deposits are stratified with more rigid water-ice bounding layers [6], and therefore, the rheology of this ice must be included in future versions of the model.

Acknowledgements: We gratefully acknowledge financial support by a NSERC Canada Research Chair.

References: [1] Clark, B. R., and R. P. Mullin (1976), *Icarus*, *27*(2), 215–228. [2] Durham, W. B. *et al.* (1999), *GRL 26*(23), 3493–3496. [3] Nye, J. F., *et al*. (2000), *Icarus*, *144*(2), 449–455. [4] Kreslavsky, M. A., and J. W. Head (2011) *Icarus*, *216*(1), 111–115. [5] Phillips, R. J. et al. (2011) *Science*, *332*(6031), 838–841. [6] Bierson, C. J. *et al.* (2016) *GRL*, *43*(9), 4172–4179. [7] Putzig et al., (2018) Icarus 308, 138–147. [8] Cross, A. J. et al., (2019) LPSC abst. 2587. [9] Smith et al., (2001) JGR 106. [10] Context Imager mosaic produced by Peter Thomas. [10] Larour, E., *et al.* (2012) *JGR Earth Surf.*, *117*(F1), F01022.